The Kerr Trisector Closure

A Self-Consistency Test of General Relativity

Tanha Aronno Mirdha und Malte Mülhenfeld
Gymnasium Heißen, Mülheim an der Ruhr, Germany
aronnomirdha@outlook.com, malte.muehlenfeld@outlook.de

Jugend forscht 2026

Abstract

General Relativity describes gravity as the geometry of spacetime. According to the theory, all observable effects caused by gravity should be explained by a single spacetime description. However, most existing tests of General Relativity study different physical effects separately and do not directly check whether they are mutually consistent. In this project we introduce the *Kerr Trisector Closure (KTC)*, a method that tests the internal consistency of spacetime geometry around a black hole. The method compares independent measurements of a black hole's mass and spin obtained from three different observational sectors: orbital motion, gravitational-wave ringdown, and black-hole imaging. If General Relativity is correct, all three measurements must agree within their experimental uncertainties. We formulate a mathematical closure statistic that quantifies the level of agreement between the sectors. Using simulated data, we demonstrate that the method behaves correctly: it does not falsely signal inconsistencies when all measurements are consistent, and it reliably detects deviations when one sector is inconsistent. The Kerr Trisector Closure provides a simple and model-independent way to test whether different observations of a black hole describe the same spacetime geometry.

1 Introduction

General Relativity describes gravity as the curvature of spacetime. Mass and energy bend spacetime, and this curvature determines how objects move, how light travels, and how time passes. In this picture, gravity is not a force, but a geometric property of spacetime itself. Over the past century, many experiments and observations have confirmed individual predictions of General Relativity. The motion of planets agrees with theory, gravitational waves from merging black holes have been detected, and images of black hole shadows have been produced. Each of these observations supports General Relativity within its own physical domain. However, these tests are usually performed separately. Orbital motion, gravitational waves, and black hole imaging are analyzed independently, even though they are all governed by the same spacetime geometry. As a result, existing tests do not directly check whether all observations of a single black hole are mutually consistent with one and the same spacetime description. This project addresses this missing consistency check. It asks a simple but fundamental question:

> *Do different observations of the same black hole all describe the same spacetime geometry, as predicted by General Relativity?*

2 The Kerr Spacetime

In General Relativity, gravity is not a force. Instead, mass and energy curve spacetime, and objects move along paths determined by this curvature. A black hole is therefore described not as a solid object, but as a particular structure of spacetime itself. An uncharged and rotating black hole is described by the *Kerr solution*. This solution represents the spacetime geometry outside the black hole, including the region where matter moves, gravitational waves are emitted, and light is bent. Remarkably, the Kerr spacetime depends on only two physical parameters: the mass M and the dimensionless spin χ. The mass determines how strongly spacetime is curved, while the spin describes how fast the black hole rotates and how strongly it drags spacetime around with it.

The dimensionless spin is defined as

$$\chi = \frac{J}{M^2}, \qquad |\chi| \leq 1, \tag{1}$$

where J is the angular momentum of the black hole. Here J and M are expressed in geometric units, so that the spin parameter χ is dimensionless. The upper limit $|\chi| = 1$ corresponds to the maximum rotation allowed by General Relativity. All physical processes outside the black hole, such as the motion of particles, the emission of gravitational waves, and the paths of light rays, are completely determined by the values of M and χ. If these two parameters are known, the external spacetime geometry is fixed. Throughout this work we use geometric units, in which the gravitational constant and the speed of light are set to one ($G = c = 1$).

3 Three Ways to Measure the Same Spacetime

A black hole cannot be observed directly. Instead, its spacetime geometry is studied through the effects it has on matter, radiation, and the motion of light. Different observations therefore measure different physical consequences of the same spacetime. In this project we consider three independent ways to measure the geometry around a black hole. Each method probes a different physical process, but all of them are governed by the same Kerr spacetime.

3.1 Orbital Motion (Dynamical Sector)

The curvature of spacetime determines how massive objects move. When two compact objects orbit each other, their motion follows the geometry of the surrounding spacetime. In close binary systems, this motion produces gravitational waves. As the objects spiral together, the frequency and shape of the gravitational-wave signal change in a precise way. This evolution depends on the mass and spin of the black hole, because these quantities control how spacetime is curved. By analyzing the gravitational-wave signal from the inspiral, we can determine an estimate of the spacetime parameters,

$$(M_{\rm dyn}, \chi_{\rm dyn}). \tag{2}$$

3.2 Ringdown Oscillations (Perturbative Sector)

After a black hole is formed or disturbed, it does not settle down immediately. Instead, it undergoes a short phase of oscillation while returning to a stable state. This process is called the ringdown. The ringdown behaves like a damped vibration, similar to the sound of a struck bell. The frequencies and decay times of these oscillations depend only on the mass and spin of the black hole. They are independent of how the black hole was formed. By measuring the ringdown signal, we obtain a second, independent estimate of the spacetime,

$$(M_{\rm rd}, \chi_{\rm rd}). \tag{3}$$

3.3 Light Paths and Imaging (Optical Sector)

Light does not travel in straight lines near a black hole. Instead, its path is bent by the strong curvature of spacetime. Some light rays can even orbit the black hole before escaping. This behavior creates visible features, such as the dark shadow surrounded by a bright photon ring. High-resolution images can measure the size and shape of these features.

From black-hole imaging, we obtain a third estimate of the spacetime parameters,

$$(M_{\rm img}, \chi_{\rm img}). \tag{4}$$

4 Hypothesis

This project is based on a single, testable hypothesis. General Relativity predicts that gravity is fully described by the geometry of spacetime. For a black hole, this means that all observable effects outside the black hole are governed by one spacetime solution. Our hypothesis is therefore:

If General Relativity correctly describes gravity, then independent measurements of a black hole's mass and spin obtained from orbital motion, ringdown oscillations, and black-hole imaging are statistically consistent with a single Kerr spacetime.

In practice, the measurements will not be exactly identical, because all observations have uncertainties. The hypothesis is considered valid as long as the differences between the measurements can be explained by these uncertainties. If, however, at least one measurement disagrees with the others by more than expected from experimental uncertainty, the hypothesis is violated. Such a result would indicate that the different observations do not describe the same spacetime geometry.

5 The Kerr Trisector Closure Method

The Kerr Trisector Closure (KTC) is a way to see if different observations of the same black hole describe the same spacetime geometry. In General Relativity, the structure of spacetime itself determines all physical effects that gravity has. The Kerr spacetime describes the structure of a black hole. It only depends on the black hole's mass and spin. This means that all observable effects, like the movement of matter, the release of gravitational waves, and the bending of light, should be controlled by the same spacetime. In real life, these effects are seen in very different ways. Different physical processes and tools are used by each observational sector to measure the black hole's mass and spin. Because of this, each measurement has its own uncertainties, and the values that are inferred will never be exactly the same. The Kerr Trisector Closure is meant to find out if the differences between these measurements are normal experimental uncertainty or if they are too big to be explained this way. If the differences are small enough, all the observations can be seen as describing the same Kerr spacetime. If the differences are too big, it means that at least one observation doesn't fit with the others, which means that spacetime consistency is breaking down.

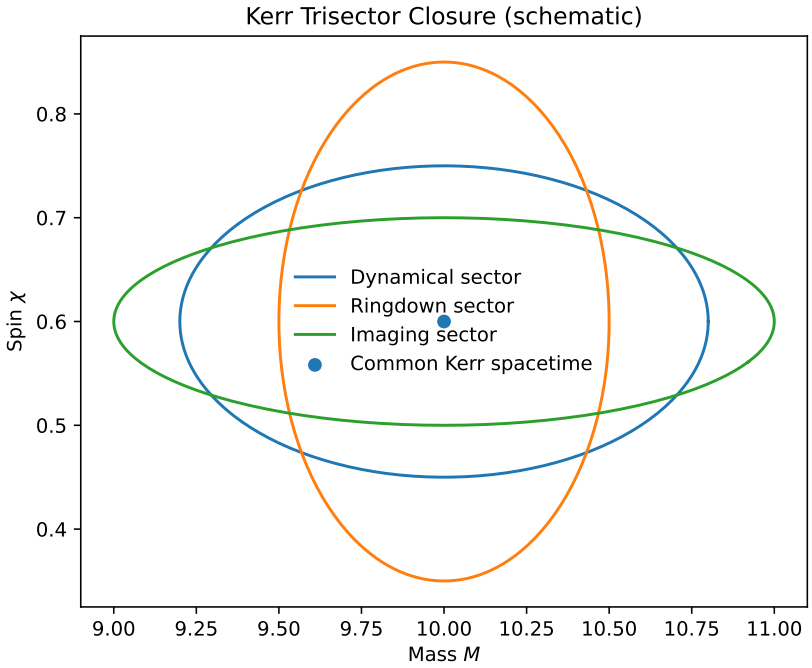

Figure 1: Schematic illustration of the Kerr Trisector Closure. Each ellipse represents the uncertainty region of a mass–spin measurement obtained from a different observational sector: orbital motion (dynamical), ringdown oscillations, and black-hole imaging. If all three sectors describe the same spacetime, their uncertainty regions overlap near a single point (the common Kerr spacetime). The closure test quantifies whether such agreement exists.

5.1 Parameter Estimates from Each Sector

We describe the spacetime of a black hole by the parameter vector

$$\Theta = (M, \chi), \tag{5}$$

where M is the mass and χ is the dimensionless spin.

Each observational sector produces an independent estimate of these parameters:

$$\hat{\Theta}_{\rm dyn} = (M_{\rm dyn}, \chi_{\rm dyn}), \tag{6}$$

$$\hat{\Theta}_{\rm rd} = (M_{\rm rd}, \chi_{\rm rd}), \tag{7}$$

$$\hat{\Theta}_{\rm img} = (M_{\rm img}, \chi_{\rm img}). \tag{8}$$

These estimates are accompanied by uncertainties, which we represent by covariance matrices $\Sigma_{\rm dyn}$, $\Sigma_{\rm rd}$, and $\Sigma_{\rm img}$. Each covariance matrix describes how precisely the corresponding sector can measure M and χ.

5.2 The Common Best-Fit Spacetime

If all observations describe the same Kerr spacetime, there should exist a single parameter pair

$$\bar{\Theta} = (\bar{M}, \bar{\chi}) \tag{9}$$

that is consistent with all three measurements. We determine this common best-fit spacetime by choosing the values of $\bar{\Theta}$ that minimize the total squared deviation from the three sector estimates, while taking their uncertainties into account. In simple terms, the best-fit spacetime lies closest to all three measurements at the same time.

5.3 Defining the Closure Probe

To test whether the measurements are consistent, we first define the deviation of each sector from the common best-fit spacetime:

$$\delta\Theta_k = \hat{\Theta}_k - \bar{\Theta}, \qquad k \in \{\rm dyn, rd, img\}. \tag{10}$$

These deviation vectors tell us how far each measurement lies from the shared Kerr spacetime.

We now combine all deviations into a single quantity, called the *closure statistic*,

$$T^2 = \sum_k \delta\Theta_k^{\rm T} \Sigma_k^{-1} \delta\Theta_k. \tag{11}$$

This quantity T^2 is the mathematical probe used in the Kerr Trisector Closure. It measures the total inconsistency between the three measurements, while properly accounting for their uncertainties.

The closure statistic T^2 has a direct physical meaning. It measures how different the three measurements of mass and spin are from one another, while taking their uncertainties into account. If the value of T^2 is small, the differences between the measurements can be explained by experimental uncertainty. In this case, all observations are consistent with a single Kerr spacetime, and the spacetime is said to be *closed*. If the value of T^2 is large, the differences between the measurements are too large to be explained by uncertainty alone. This indicates that at least one observational sector does not agree with the others, and the spacetime description is no longer consistent. In this method we compare three independent measurements of two physical parameters. This leaves four independent degrees of freedom. For this reason, if all measurements describe the same Kerr spacetime, the closure statistic T^2 follows a chi-squared distribution with four degrees of freedom. If the observed value of T^2 exceeds the range expected from this distribution, the hypothesis of a single Kerr spacetime is rejected.

6 Demonstration Using Simulated Data

At the moment, one and the same astrophysical black hole has not yet been measured with high precision in all three sectors at once (orbital motion, ringdown, and imaging). Because of this, we first test the *method itself* using simulated data. In this work we assume that the measurement errors of the three

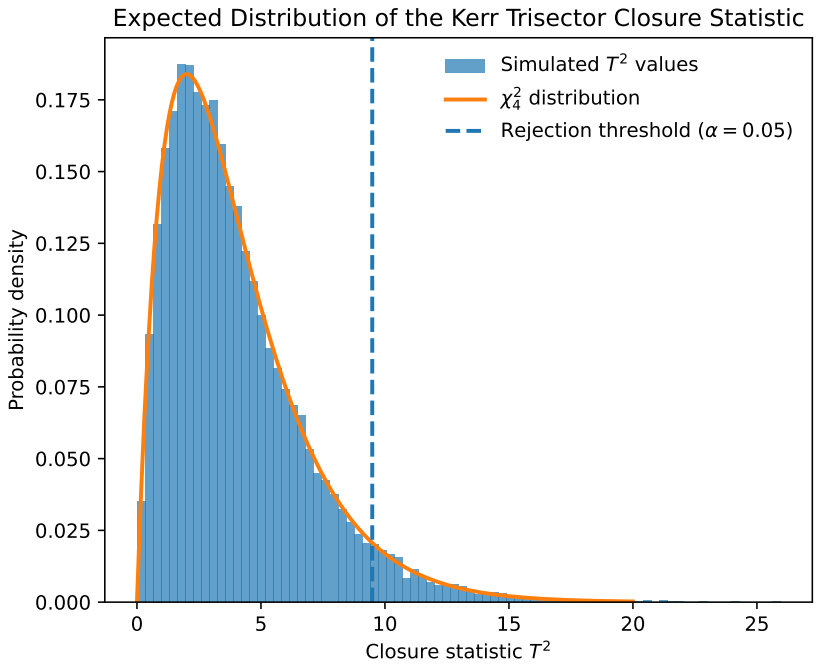

Figure 2: Distribution of the Kerr Trisector Closure statistic T^2 obtained from simulated, mutually consistent measurements. The solid curve shows the theoretical chi-squared distribution with four degrees of freedom. The dashed line marks the rejection threshold at the 5% level. Values of T^2 to the right of this line indicate a statistically significant inconsistency.

observational sectors are statistically independent. The goal of this demonstration is simple: we want to check that the Kerr Trisector Closure behaves in the right way.

Idea of the simulation. We start by choosing a "true" black hole spacetime with fixed parameters

$$\Theta^* = (M^*, \chi^*). \tag{12}$$

Then we generate three independent "measurements" of Θ^*, one from each sector. Each measurement contains random error, because real experiments are noisy. If General Relativity is consistent across the three sectors, these errors should be enough to explain small differences between sectors. If we artificially add a bias in one sector, the closure statistic should detect it.

Mathematical model for one simulated measurement. For each sector $k \in \{\mathrm{dyn}, \mathrm{rd}, \mathrm{img}\}$, we simulate a measured parameter vector

$$\hat{\Theta}_k = \Theta^* + \varepsilon_k, \tag{13}$$

where the measurement error ε_k is a two-dimensional random vector. We assume it is Gaussian-distributed with mean zero and covariance matrix Σ_k:

$$\varepsilon_k \sim \mathcal{N}(0, \Sigma_k). \tag{14}$$

This Gaussian approximation is valid when the measurements are close to the best-fit solution, which is the regime relevant for consistency tests. The assumption is a standard first approximation: near the best-fit solution, many measurement uncertainties behave roughly like a Gaussian distribution.

For simplicity in this demonstration, we take the covariance matrices to be diagonal, meaning we treat the mass and spin errors as uncorrelated:

$$\Sigma_k = \begin{pmatrix} \sigma^2_{M,k} & 0 \\ 0 & \sigma^2_{\chi,k} \end{pmatrix}. \tag{15}$$

(The KTC method also works with non-diagonal Σ_k; the diagonal case is just easier to explain and already demonstrates the main idea.)

Step 1: Compute the common best-fit spacetime. From the three measurements $\hat{\Theta}_k$ we compute one common best-fit pair $\bar{\Theta} = (\bar{M}, \bar{\chi})$. It is defined as the value of Θ that minimizes the weighted disagreement

$$\chi^2(\Theta) = \sum_k (\hat{\Theta}_k - \Theta)^{\mathrm{T}} \Sigma_k^{-1} (\hat{\Theta}_k - \Theta). \tag{16}$$

Note that $\chi^2(\Theta)$ is used only to compute the best-fit parameters, while T^2 is the closure statistic used for the consistency test. This is a weighted version of "finding the best average": measurements with smaller uncertainty (smaller Σ_k) are trusted more.

The minimum can be written explicitly as

$$\bar{\Theta} = \left(\sum_k \Sigma_k^{-1} \right)^{-1} \left(\sum_k \Sigma_k^{-1} \hat{\Theta}_k \right). \tag{17}$$

Step 2: Compute the closure statistic. We define the deviation of each sector from the common best-fit spacetime as

$$\delta\Theta_k = \hat{\Theta}_k - \bar{\Theta}. \tag{18}$$

The Kerr Trisector Closure probe is then the closure statistic

$$T^2 = \sum_k \delta\Theta_k^{\mathrm{T}} \Sigma_k^{-1} \delta\Theta_k. \tag{19}$$

This number is small when all three sectors agree within their uncertainties, and it becomes large when one sector disagrees too strongly.

Why the degrees of freedom are 4. We have 3 sectors and each gives 2 numbers (M, χ), so in total there are 6 measured values. We fit 2 common parameters $(\bar{M}, \bar{\chi})$. That leaves $6 - 2 = 4$ independent "leftover" pieces of information. Therefore, if all measurements are consistent with a single Kerr spacetime, the statistic T^2 follows a chi-squared distribution with 4 degrees of freedom.

Test A: Consistent (GR-like) data should not trigger false alarms. We generate many simulated triples $(\hat{\Theta}_{\mathrm{dyn}}, \hat{\Theta}_{\mathrm{rd}}, \hat{\Theta}_{\mathrm{img}})$ using the model above and compute T^2 each time. For a significance level $\alpha = 0.05$ (5%), the rejection threshold is the 95% quantile of χ^2_4,

$$T^2 > \chi^2_{4,\,0.95} \approx 9.49. \tag{20}$$

In a correct method, only about 5% of perfectly consistent datasets should exceed this threshold (these are statistical fluctuations).

In an example Monte-Carlo test with $N = 200{,}000$ simulated datasets, we obtained

$$\langle T^2 \rangle \approx 4.00, \qquad \Pr(T^2 > 9.49) \approx 0.050, \tag{21}$$

which matches the expected behaviour of χ^2_4 very closely. This shows that the KTC does not falsely claim an inconsistency when the sectors are consistent by construction.

Test B: A controlled inconsistency should be detected. Next we introduce an artificial, systematic shift in one sector. For example, we modify only the imaging sector by adding a fixed bias vector Δ:

$$\hat{\Theta}_{\mathrm{img}} = \Theta^* + \Delta + \varepsilon_{\mathrm{img}}, \tag{22}$$

while keeping the other two sectors unchanged,

$$\hat{\Theta}_{\mathrm{dyn}} = \Theta^* + \varepsilon_{\mathrm{dyn}}, \qquad \hat{\Theta}_{\mathrm{rd}} = \Theta^* + \varepsilon_{\mathrm{rd}}. \tag{23}$$

Now the three sectors no longer describe the same spacetime, so the closure statistic should become larger and exceed the threshold more often. In an example where we injected a moderate bias in the imaging sector, we found that T^2 shifted strongly to larger values and crossed the 5% threshold in a large fraction of the simulated datasets. This demonstrates that the KTC is sensitive to inconsistencies that cannot be explained by measurement uncertainty.

Identifying the deviating sector. To see which sector causes the inconsistency, we also compute the individual sector contributions

$$T_k^2 = \delta\Theta_k^{\mathrm{T}} \Sigma_k^{-1} \delta\Theta_k, \qquad T^2 = T^2_{\mathrm{dyn}} + T^2_{\mathrm{rd}} + T^2_{\mathrm{img}}. \tag{24}$$

In the injected-bias test, the largest contribution typically comes from the sector where the bias was introduced, which provides a clear diagnostic of the problem.

Overall, these simulations show that the Kerr Trisector Closure behaves correctly: it stays quiet when all sectors are consistent, and it reacts strongly when a real inconsistency is present.

Figure 3: Schematic illustration of a failed Kerr Trisector Closure. The uncertainty regions obtained from the three observational sectors do not overlap. Such a configuration leads to a large closure statistic T^2 and indicates that the observations cannot be described by a single Kerr spacetime.

7 Discussion

The Kerr Trisector Closure not only checks if the spacetime description is consistent, but it also tells us where a possible inconsistency might be coming from. If a big difference is found, the differences from the normal Kerr spacetime don't have to be evenly spread out across all observational sectors. One sector, on the other hand, may disagree much more strongly than the others. So, the way these deviations happen can help us figure out where the problem came from in the real world. If the biggest difference is in the dynamic sector, it means that the Kerr solution's spacetime geometry doesn't match the way big things move. If this happened, it would mean that the way orbits work or the way gravity waves travel would need to be changed. If the main deviation shows up in the ringdown sector, it means that the black hole's oscillation frequencies don't match what the Kerr prediction says they should be. The ringdown is sensitive to the area near the event horizon, so this difference would point to new effects in the spacetime near the horizon. If the inconsistency is strongest in the imaging sector, it means that the way light travels near the black hole doesn't match the expected Kerr geometry. This could mean that the way light moves through strongly curved spacetime has changed. Lastly, if all three sectors show big, similar differences, the inconsistency can't be blamed on just one physical process. In this case, the most likely explanation is that the Kerr description itself is broken down, which means that a single Kerr metric can't describe the external spacetime.

8 Conclusion

In this project we introduced the Kerr Trisector Closure, a method designed to test whether different observations of the same black hole describe a single, consistent spacetime geometry, as predicted by General Relativity. The method is based on a simple idea: if gravity is fully described by spacetime geometry, then independent measurements of a black hole's mass and spin obtained from different physical processes must agree within their experimental uncertainties. We applied this idea to three observational sectors: orbital motion, gravitational-wave ringdown, and black-hole imaging. We formulated a closure statistic that quantitatively measures the level of agreement between these sectors. Using simulated data, we demonstrated that the method behaves as intended. When all measurements are consistent by construction, the closure statistic remains within the expected statistical range. When an artificial

inconsistency is introduced in one sector, the method reliably detects the deviation and identifies its origin. The Kerr Trisector Closure provides a model-independent way to test the internal consistency of spacetime geometry without assuming any specific modification of General Relativity. While current observations do not yet allow a full experimental application of the method, future gravitational-wave detectors and high-resolution black-hole imaging experiments may make such tests possible. Overall, this work shows that the idea of spacetime consistency can be turned into a concrete and testable criterion. Whether confirmed or violated by future observations, the Kerr Trisector Closure offers a clear framework for probing the geometric foundations of gravity.

References

[1] L. Barack and C. Cutler. Using lisa emri sources to test off-kerr deviations in the geometry of massive black holes. *Phys. Rev. D*, 75:042003, 2007.

[2] E. Barausse, N. Yunes, and K. Chamberlain. Theory-independent tests of general relativity with gravitational waves. *Phys. Rev. Lett.*, 116:241104, 2016.

[3] E. Berti, V. Cardoso, and A. O. Starinets. Quasinormal modes of black holes and black branes. *Class. Quantum Grav.*, 26:163001, 2009.

[4] V. Cardoso, E. Franzin, and P. Pani. Is the gravitational-wave ringdown a probe of the event horizon? *Phys. Rev. Lett.*, 116:171101, 2016.

[5] Event Horizon Telescope Collaboration. First m87 event horizon telescope results. i. the shadow of the supermassive black hole. *Astrophys. J. Lett.*, 875(1):L1, 2019.

[6] Event Horizon Telescope Collaboration. First sagittarius a* event horizon telescope results. i. the image of the supermassive black hole in the center of the milky way. *Astrophys. J. Lett.*, 930(2):L12, 2022.

[7] Event Horizon Telescope Collaboration. Tests of general relativity with the 2017 event horizon telescope observations of m87*. *Astrophys. J. Lett.*, 930(2):L17, 2022.

[8] S. Datta, A. Ghosh, and P. Ajith. Testing the binary black hole nature of gravitational-wave signals from the ringdown phase. *Phys. Rev. D*, 108:064036, 2023.

[9] A. Einstein. Die feldgleichungen der gravitation. *Sitzungsberichte der Königlich Preussischen Akademie der Wissenschaften*, pages 844–847, 1915.

[10] A. E. Broderick et al. The photon ring in m87* and tests of general relativity at the horizon scale. *Astrophys. J.*, 935(1):61, 2022.

[11] A. Ghosh et al. Testing general relativity using golden black-hole binaries. *Phys. Rev. D*, 97:104060, 2018.

[12] D. Psaltis et al. Gravitational test beyond the first post-newtonian order with the shadow of the m87 black hole. *Phys. Rev. Lett.*, 125:141104, 2020.

[13] E. Berti et al. Testing general relativity with present and future astrophysical observations. *Class. Quantum Grav.*, 32:243001, 2015.

[14] G. Carullo et al. Evidence for the post-merger phase of gw150914 in the ligo livingston detector. *Phys. Rev. D*, 100:104036, 2019.

[15] M. D. Johnson et al. The next-generation event horizon telescope: Science case and key goals. *Astrophys. J.*, 943(2):L33, 2023.

[16] M. Evans et al. A horizon study for cosmic explorer: Science, observatories, and community. *arXiv preprint*, 2021.

[17] M. Punturo et al. The einstein telescope: A third-generation gravitational wave observatory. *Class. Quantum Grav.*, 27:194002, 2010.

[18] P. T. H. Pang et al. A numerical relativity waveform surrogate model for binary black hole coalescence beyond the ringdown. *Phys. Rev. D*, 104:104054, 2021.

[19] B. P. Abbott et al. (LIGO Scientific Collaboration and Virgo Collaboration). Observation of gravitational waves from a binary black hole merger. *Phys. Rev. Lett.*, 116(6):061102, 2016.

[20] B. P. Abbott et al. (LIGO Scientific Collaboration and Virgo Collaboration). Tests of general relativity with the binary black hole signals from the first and second observing runs of advanced ligo and advanced virgo. *Phys. Rev. D*, 100:104036, 2019.

[21] P. Amaro-Seoane et al. (LISA Consortium). Laser interferometer space antenna. *arXiv preprint*, 2017.

[22] J. R. Gair, M. Vallisneri, S. L. Larson, and J. G. Baker. Testing general relativity with low-frequency, space-based gravitational-wave detectors. *Living Rev. Relativity*, 16(7), 2013.

[23] S. A. Hughes. Trust but verify: The case for testing extreme-mass-ratio inspirals as probes of strong-field gravity. *Phys. Rev. D*, 81:064018, 2010.

[24] M. Isi and W. M. Farr. Hierarchical tests of general relativity with gravitational waves. *Phys. Rev. D*, 104:044037, 2021.

[25] M. Isi, M. Giesler, W. M. Farr, M. A. Scheel, and S. A. Teukolsky. Testing the no-hair theorem with gw150914. *Phys. Rev. Lett.*, 123:111102, 2019.

[26] T. Johannsen. Photon rings around kerr and kerr-like black holes. *Astrophys. J.*, 777(2):170, 2013.

[27] R. P. Kerr. Gravitational field of a spinning mass as an example of algebraically special metrics. *Phys. Rev. Lett.*, 11:237–238, 1963.

[28] E. W. Leaver. An analytic representation for the quasi-normal modes of kerr black holes. *Proc. R. Soc. Lond. A*, 402:285–298, 1985.

[29] C. W. Misner, K. S. Thorne, and J. A. Wheeler. *Gravitation*. W. H. Freeman, San Francisco, 1973.

[30] P. Pani and V. Cardoso. Are black holes in alternative theories serious astrophysical candidates? the example of einstein–dilaton–gauss–bonnet gravity. *Phys. Rev. D*, 79:084031, 2009.

[31] W. H. Press. Long wave trains of gravitational waves from a vibrating black hole. *Astrophys. J. Lett.*, 170:L105, 1971.

[32] T. Regge and J. A. Wheeler. Stability of a schwarzschild singularity. *Phys. Rev.*, 108:1063–1069, 1957.

[33] L. Rezzolla and A. Zhidenko. New parametrization for spherically symmetric black holes in metric theories of gravity. *Phys. Rev. D*, 90:084009, 2014.

[34] B. S. Sathyaprakash and B. F. Schutz. Physics, astrophysics, and cosmology with gravitational waves. *Living Rev. Relativity*, 12(2), 2009.

[35] J. D. Schnittman. Astrophysics of extreme-mass-ratio inspirals. *Class. Quantum Grav.*, 35(10):104002, 2018.

[36] S. A. Teukolsky. Perturbations of a rotating black hole. i. fundamental equations for gravitational, electromagnetic, and neutrino-field perturbations. *Astrophys. J.*, 185:635–648, 1973.

[37] C. V. Vishveshwara. Scattering of gravitational radiation by a schwarzschild black-hole. *Nature*, 227:936–938, 1970.

[38] C. M. Will. The confrontation between general relativity and experiment. *Living Rev. Relativity*, 17(4), 2014.

[39] N. Yunes and F. Pretorius. Fundamental theoretical bias in gravitational-wave astrophysics and the parameterized post-einsteinian framework. *Phys. Rev. D*, 80:122003, 2009.